International Journal of GEOMATE, May, 2026 Vol.30, Issue 141, pp. 112-120
ISSN: 2186-2982 (P), 2186-2990 (O), Japan, DOI: https://doi.org/10.21660/2026.141.g15172
Geotechnique, Construction Materials and Environment

SUSTAINABLE UTILIZATION OF COAL BOTTOM ASH AS AN ADDITIVE IN FIRED CLAY BRICK PRODUCTION

Nonthaphong Phonphuak[1], Anuwat Srisuwan[2], Anujit Phumiphan[3], Sibpawishkon Sittiakkaranon[4] and *Siwat Lawanwadeekul[5]

[1] Faculty of Engineering, Rajabhat Maha Sarakham University, 44000, Thailand
[2] Faculty of Liberal Art and Science, Sisaket Rajabhat University, Muang, Sisaket 33000, Thailand
[3]School of Engineering University of Phayao, Phayao 56000, Thailand
[4] Faculty of Agricultural and Industrial Technology, Rajabhat Nakhon Sawan University, Thailand
[5] Faculty of Industrial Technology, Lampang Rajabhat University, Lampang 52100, Thailand

*Corresponding author, Received: 27 May 2025, Revised: 24 Jan. 2026, Accepted: 30 Jan. 2026

ABSTRACT: The accumulation of coal bottom ash (CBA) poses environmental concerns, creating a need for sustainable recycling routes. This study investigates the feasibility of using CBA as a supplementary raw material in fired clay bricks. Specimens containing 0–40 wt.% CBA were fabricated and fired at 900, 1000, and 1100 °C. The effects of CBA incorporation on physical properties, compressive strength, and microstructural evolution were systematically evaluated. Increasing CBA content decreased bulk density and compressive strength while increasing apparent porosity and water absorption. SEM observations indicated that pore formation was mainly induced by sulfate decomposition and residual carbon combustion during firing. Raising the firing temperature promoted densification through flux-assisted liquid-phase sintering. XRD results highlighted the formation of albite from alkali-rich CBA and the presence of inherited mullite, which together influenced the sintering behavior and structural stability of the bricks. Bricks containing 10–30 wt.% CBA fired at ≥1000 °C achieved compressive strengths above 17.2 MPa, satisfying ASTM C62 requirements for moderate weathering (MW) conditions. The findings confirm that controlled CBA incorporation can produce durable, eco-friendly masonry bricks and support circular-economy-based resource utilization.

Keywords: Coal Bottom Ash, Fired Clay Bricks, Waste Valorization, Microstructure, Sintering

1. INTRODUCTION

The construction materials sector is pivotal in addressing global challenges related to solid waste management and resource depletion. A strategy that has gained increasing traction is the integration of industrial by-products and post-consumer waste into standard building materials, thereby supporting resource efficiency and circular economy principles [1,2]. Fired clay bricks are particularly suitable for this type of waste valorization, as their manufacturing process can tolerate compositional variations without detrimentally affecting fundamental performance. By substituting a portion of natural clay with appropriate waste materials, manufacturers can minimize the extraction of virgin resources, reduce landfill usage, and potentially lower production costs [3,4]. These advantages align with the rising demand for sustainable construction, encouraging the adoption of waste-derived materials provided they meet relevant technical standards [5,6].

Despite these benefits, traditional brick manufacturing remains a significant source of environmental pollution. The energy-intensive firing process and the combustion of fossil fuels release substantial greenhouse gases (GHGs) and air pollutants, contributing to smog, acid rain, and global warming [7]. Consequently, researchers have increasingly focused on finding alternative raw materials that can partially replace natural clay, thereby mitigating the environmental footprint associated with its extraction and firing [8,9]. Since fired clay bricks are typically sintered at temperatures between 900 and 1100 °C, their physical and mechanical properties are heavily dependent on raw material composition and the sintering regime [10]. Therefore, incorporating industrial by-products requires careful optimization to ensure that the durability and strength of the final product remain within acceptable limits [11].

Among various industrial residues, coal bottom ash (CBA) has emerged as a promising candidate for clay replacement. CBA is a coarse, granular by-product formed at the bottom of boilers in coal-fired power plants. Large volumes of CBA are generated annually, often leading to stockpiling or landfilling, which raises environmental and land-use concerns [3]. However, its chemical composition—typically rich in SiO_2 and Al_2O_3, along with fluxing oxides like CaO—suggests that CBA can effectively participate in ceramic sintering reactions [12]. As a result, CBA has been explored in various civil engineering applications, ranging from road bases and backfills to cementitious binders and, more recently, fired bricks.

Prior studies indicate that incorporating bottom ash into brick mixtures significantly affects both the

microstructure and macroscopic properties of the fired products. Adediran et al. reported that adding bottom ash to illitic clay improved apparent density and compressive strength while reducing crack formation and water absorption, attributing these benefits to alkali oxides that facilitate liquid-phase formation and vitrification [13]. Conversely, Kizinievič et al. found that municipal solid waste incineration bottom ash reduced drying shrinkage but increased porosity, thereby lowering mechanical strength [14]. Furthermore, Sutcu et al. demonstrated that bricks containing bottom ash and fly ash fired at 1050 °C had lower porosity and water absorption than those fired at lower temperatures. However, these improvements were generally limited to low ash contents of 5–10 wt.% [15]. Collectively, these findings suggest that while CBA is a viable partial replacement for clay, the resulting brick properties are strongly influenced by ash content, mineralogy, and specific firing conditions.

2. RESEARCH SIGNIFICANCE

This study addresses a critical knowledge gap regarding the combined influence of coal bottom ash (CBA) content and firing temperature on the performance of fired clay bricks, by systematically evaluating specimens with up to 40 wt.% CBA under industrially relevant sintering regimes (900–1100 °C) and interpreting the results against ASTM C62-23 requirements, this work establishes practical guidelines for manufacturing durable, eco-friendly masonry units. In particular, the study elucidates the interplay between pore-forming mechanisms, flux-assisted liquid-phase sintering, and phase evolution as a function of CBA dosage and firing temperature, providing a mechanistic basis for optimizing brick formulations. The findings provide a validated pathway to valorize coal-combustion by-products, thereby promoting resource efficiency, reducing the environmental footprint of the construction industry, and supporting the broader implementation of circular-economy strategies in ceramic and construction materials engineering.

3. MATERIALS AND METHODS

3.1 Materials

In this study, two primary raw materials were utilized to fabricate the brick specimens. The base material was natural clay, acquired from a local brick manufacturing plant in Kamala Sai District, Kalasin Province, Thailand (Fig. 1(a)). As a supplementary additive, coal bottom ash (CBA) was sourced from the Mae Moh coal-fired power plant in Lampang Province, Thailand (Fig. 1(b)).

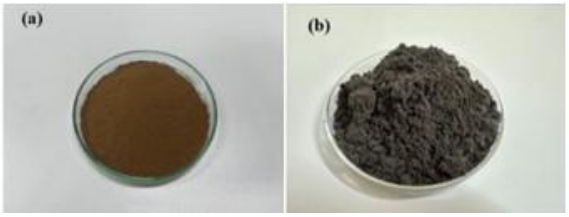

Fig. 1 Raw materials: (a) natural clay and (b) coal bottom ash (CBA).

The chemical and physical properties of these raw materials were comprehensively characterized. X-ray fluorescence (XRF; Horiba, Japan) was employed to determine their oxide compositions, as summarized in Table 1. The mineralogical phases were identified by X-ray diffraction (XRD) using an X'Pert Pro MPD diffractometer (Philips, Netherlands). In addition, the particle size distribution was obtained using a laser diffraction analyzer (Mastersizer 2000 equipped with a Hydro 2000 MU dispersion unit), while the morphological features were examined with a scanning electron microscope (SEM; LEO 1460 VP, Zeiss).

Table 1. Chemical oxide composition of clay and CBA used in the experiments.

Oxide (wt.%)	Clay	CBA
SiO_2	50.49	56.22
Al_2O_3	29.84	15.76
Fe_2O_3	5.90	6.00
CaO	0.30	11.00
K_2O	1.20	1.53
Na_2O	-	-
SO_3	-	3.32
TiO_2	0.80	0.45
MnO	1.20	0.10
MgO	-	0.07
LOI.	9.34	5.56

3.2 Methods

3.2.1 Preparation of brick specimens

Brick specimens were prepared by first dry mixing the pre-dried natural clay and CBA to obtain a homogeneous blend. Water was then added at approximately 10–15 wt.% to achieve sufficient plasticity for molding (Fig. 2). The resulting mixture was manually compacted into steel molds to form rectangular specimens with nominal dimensions of 50 × 95 × 30 mm.

The green bricks were subjected to a two-stage drying regime. First, they were air-dried in ambient laboratory conditions for seven days to minimize cracking. Subsequently, the specimens were oven-dried at 110 °C for 48 h to remove residual moisture.

The dried bricks were then fired in a laboratory furnace at 900, 1000, and 1100 °C using a heating rate of 5 °C/min and a soaking time of 30 min at the target temperature to ensure thermal equilibrium throughout the specimens.

Fig. 2 Manual mixing of raw materials for clay bricks.

3.2.2 Characterization of fired bricks

The physical and mechanical properties of the fired bricks were evaluated in accordance with relevant international standards. Linear firing shrinkage was determined following ASTM C326-09 (2018) [16]. Apparent porosity, water absorption, and bulk density were measured by the Archimedes method as specified in ASTM C373-18 (2018) [17].

Compressive strength tests were performed using a universal testing machine (Chun Yen Testing Machines Co.) in accordance with ASTM C773-88 (2020) [18]. For each mixture and firing temperature, ten specimens were tested to ensure statistical reliability. The reported values represent the arithmetic mean, and standard deviations are indicated as error bars in the corresponding figures.

4. RESULTS AND DISCUSSION

4.1 Characterization of Raw Materials

The oxide compositions of the starting materials, determined by XRF, are summarized in Table 1. The natural clay is dominated by SiO_2 (50.49 wt.%) and Al_2O_3 (29.84 wt.%), with smaller quantities of fluxing oxides such as K_2O, Fe_2O_3, CaO, MnO, and TiO_2. In contrast, the coal bottom ash (CBA) contains a slightly higher silica content (56.22 wt.%) but a lower alumina fraction (15.76 wt.%) than the clay. CBA also exhibits markedly higher CaO content (11.00 wt.%), together with MgO and Fe_2O_3. This relatively high concentration of basic and fluxing oxides suggests that CBA can promote liquid-phase formation during firing, potentially lowering the effective melting temperature and enhancing vitrification of the ceramic body.

Particle size analyses performed in accordance with ASTM D422-63 (2007) [19] highlight apparent physical differences between the two raw materials (Fig. 3). The clay exhibits a relatively fine particle size distribution, with a mean diameter of 42.38 µm, consistent with its good plasticity and workability during forming. In contrast, the CBA is considerably coarser, with an average particle size of about 100 µm. This coarser, granular nature is expected to affect the packing density and the initial pore structure of the green bricks, and thus to influence the development of porosity during firing.

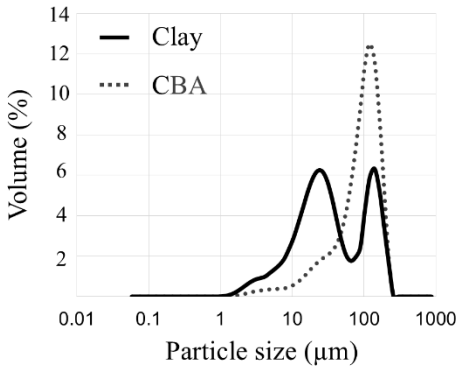

Fig. 3 Particle size distribution of the raw materials.

The mineralogical characteristics obtained from XRD patterns are shown in Fig. 4. For the clay, quartz (SiO_2) and kaolinite ($Al_2(Si_2O_5)(OH)_4$) are identified as the main crystalline phases, accompanied by minor orthoclase, hematite, and muscovite peaks. This assemblage is typical of clays used in conventional brick production. In contrast, the CBA exhibits a more complex mineralogy, including high-temperature phases such as mullite ($3Al_2O_3 \cdot 2SiO_2$) and anorthite ($CaO \cdot Al_2O_3 \cdot 2SiO_2$), together with calcite, hematite, and residual quartz. The presence of mullite and anorthite reflects the ash's prior exposure to elevated temperatures during coal combustion, and these phases can influence the sintering behavior of CBA–clay mixtures.

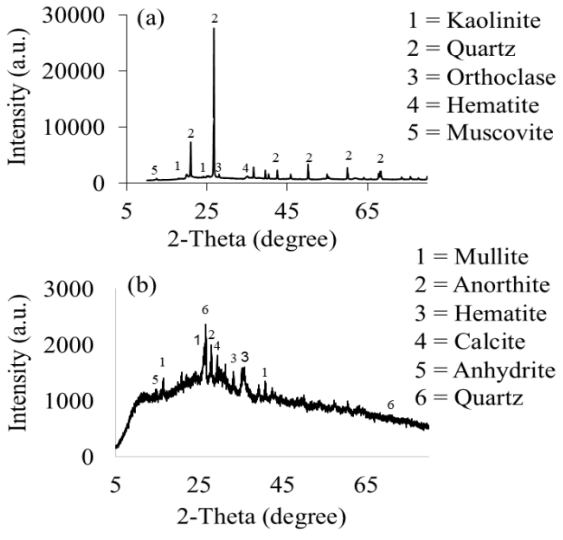

Fig. 4 XRD patterns of (a) raw clay and (b) CBA.

Microstructural observations by SEM (Fig. 5) further underline the differences between the two materials. The clay appears as agglomerated, plate-like particles typical of phyllosilicate-rich soils, whereas the CBA particles exhibit a coarser, angular, and heterogeneous morphology, often with porous or vesicular surfaces characteristic of combustion-derived residues. Such morphological features are expected to contribute to CBA's pore-forming role when incorporated into brick formulations.

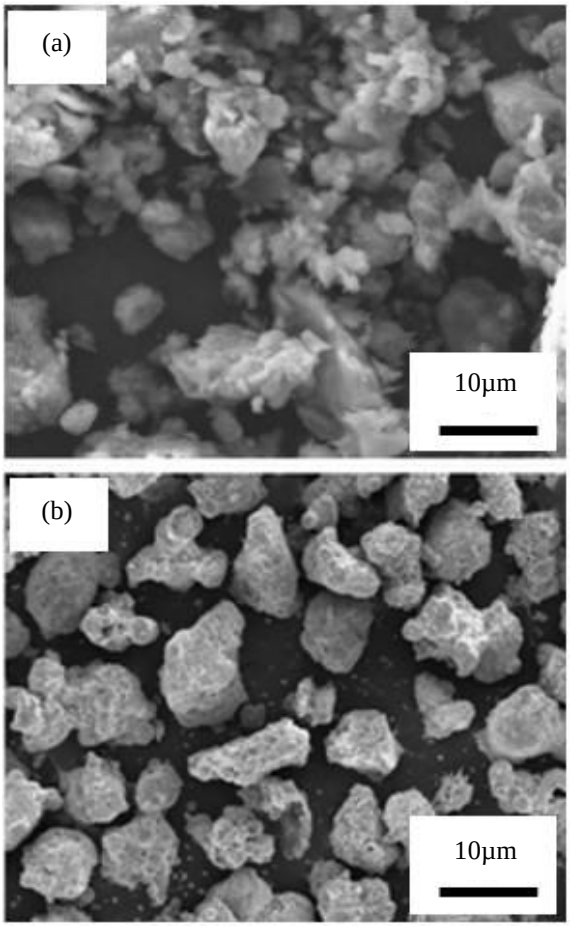

Fig. 5 SEM images of (a) raw clay and (b) CBA.

4.2 Technical properties of fired clay bricks

4.2.1 Bulk density

Bulk density of the fired bricks provides a primary indication of the degree of densification and, hence, the overall quality of the final product. As shown in Fig. 6, a clear inverse relationship is observed between CBA content and bulk density. The control bricks (0 wt.% CBA) exhibit the highest densities, increasing from 2.14 g/cm³ at 900 °C to 2.33 g/cm³ at 1100 °C. With the incorporation of CBA, bulk density progressively decreases. For example, at 1100 °C, the density drops to 2.26 g/cm³ for the mix with 10 wt.% CBA and further declines to 1.98 g/cm³ when the CBA content is increased to 40 wt.%. This behavior can be attributed to two main factors: the lower specific gravity of CBA compared with natural clay and the development of additional pores due to the combustion of residual carbon in the ash during firing [20]. In contrast, increasing the firing temperature enhances bulk density across all mixtures, reflecting improved sintering and consolidation of the ceramic matrix.

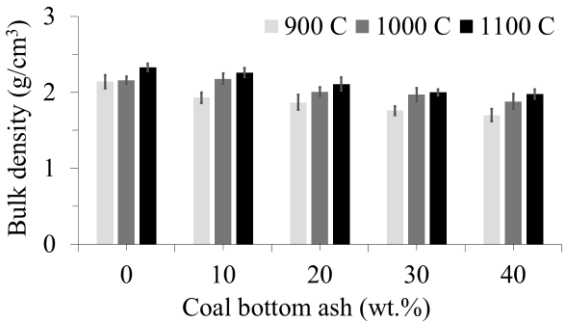

Fig. 6 Bulk density of fired clay brick samples.

4.2.2 Water absorption

Water absorption is a key durability parameter because it reflects the susceptibility of masonry units to moisture ingress and related deterioration mechanisms such as freeze–thaw damage [21]. The water absorption values of the brick specimens are presented in Fig. 7. The control bricks show the lowest absorption (8.36–13.44%), consistent with their relatively compact microstructure. Incorporation of CBA leads to higher absorption, with values in the range of 11.20–19.33% for mixtures containing 10–40 wt.% CBA. This increase is associated with the higher porosity introduced by the ash. However, raising the firing temperature significantly mitigates this effect by promoting liquid-phase formation and partial pore sealing, thereby reducing capillary connectivity and permeability [13].

According to ASTM C62-23 [26], severe-weathering (SW) grade bricks must exhibit water absorption ≤17%, whereas moderate-weathering (MW) grade bricks may have absorption up to 22%. The present results indicate that bricks containing up to 30 wt.% CBA and fired at temperatures ≥1000 °C satisfy the stringent SW requirement. This performance is attributed to enhanced vitrification and partial pore sealing induced by flux-assisted liquid-phase formation at elevated firing temperatures. This finding confirms that, under appropriate firing conditions, CBA-containing bricks

can achieve durability levels comparable to those of conventional structural bricks used in exposed environments.

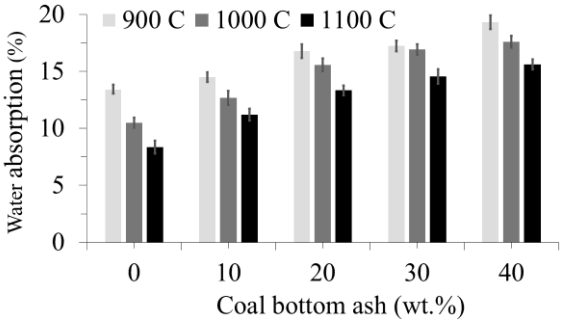

Fig. 7 Water absorption of fired clay brick samples.

4.2.3 Apparent porosity

Apparent porosity is intrinsically linked to bulk density and water absorption, and it plays an important role in governing both thermal insulation and mechanical performance [22]. As depicted in Fig. 8, porosity follows a trend opposite to that of bulk density. Increasing CBA content generally leads to higher porosity, with the maximum value of 34.95% obtained for the 40 wt.% CBA mixture fired at 900 °C. This confirms the pore-forming role of CBA in the brick body. In contrast, the lowest porosity among the modified bricks (23.43%) is recorded for the 10 wt.% CBA mixture fired at 1100 °C. The reduction in porosity at elevated firing temperatures is consistent with progressive vitrification; the formation of a glassy phase allows molten material to flow into and seal open pores, thereby densifying the microstructure and improving moisture resistance.

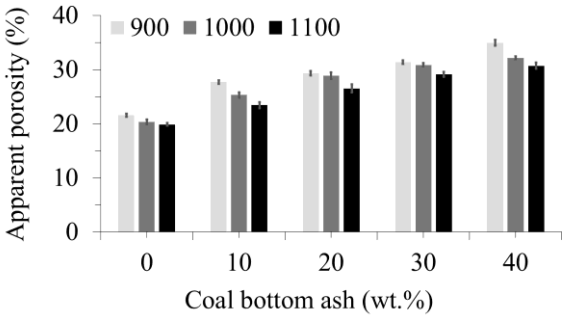

Fig. 8 Apparent porosity of fired clay brick samples.

4.2.4 Firing shrinkage

Dimensional stability is essential to ensure that finished bricks meet dimensional tolerances and can be used without causing defects in masonry assemblies. The linear firing shrinkage values shown in Fig. 9 range from 4.55% to 6.83% for all mixtures. In general, shrinkage increases with firing temperature, reflecting enhanced particle rearrangement, densification, and liquid-phase formation at higher temperatures [23,24]. Nevertheless, for all CBA contents and firing conditions, the measured shrinkage remains well below the commonly accepted 8% limit used in industrial practice and is consistent with the guidelines in ASTM C62-23 [26]. This indicates that incorporating CBA does not induce excessive deformation during firing, and the resulting bricks maintain acceptable dimensional accuracy for construction applications.

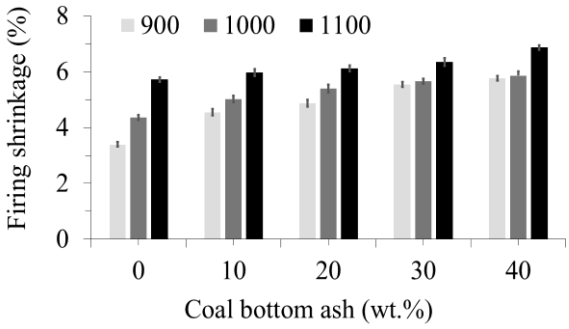

Fig. 9 Firing shrinkage of fired clay brick samples.

4.2.5 Compressive strength

Compressive strength is the most critical indicator of structural integrity and service performance of masonry units. In accordance with ASTM C62-23 [26], building bricks for moderate weathering (MW) conditions must achieve a minimum average compressive strength of 17.2 MPa. The results in Fig. 10 show a distinct inverse relationship between CBA content and compressive strength. The control bricks (0 wt.% CBA) consistently exhibit the highest strengths, reaching a maximum of 28.10 MPa when fired at 1100 °C. As CBA is incorporated, compressive strength decreases progressively; the lowest value (16.75 MPa) occurs in the 40 wt.% CBA specimens fired at 900 °C.

Despite this reduction, most CBA-modified bricks still satisfy the ASTM requirement. Mixtures containing 10–30 wt.% CBA fired at 900 °C, and those containing up to 40 wt.% CBA fired at ≥1000 °C, exceed the 17.2 MPa threshold. The strength reduction with increasing CBA is primarily associated with the formation of macropores and the corresponding decrease in bulk density, which introduces stress-concentration sites within the ceramic body [3,25]. Conversely, higher firing temperatures compensate for this effect by promoting stronger sintering, crystallization of new phases, and development of a vitreous liquid phase that bonds particles more effectively, thus enhancing the load-bearing capacity of the bricks [14].

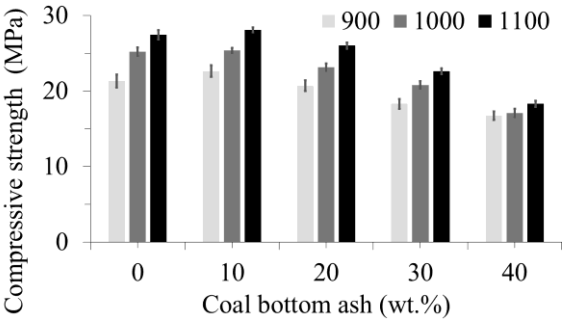

Fig. 10 Compressive strength of fired clay brick samples.

4.3 Mineralogical composition and microstructure and analysis

To further elucidate the sintering mechanisms and the microstructural changes observed in SEM, X-ray diffraction (XRD) was performed to identify the crystalline phases of the fired bricks. Fig. 11 compares diffraction patterns of the specimens grouped by firing temperature: 900 °C (Fig. 11a–c), 1000 °C (Fig. 11d–f), and 1100 °C (Fig. 11g–i).

For the control bricks (0 wt.% CBA; Fig. 11a, d, g), the major crystalline phases are quartz (SiO_2) and hematite (Fe_2O_3), accompanied by minor cristobalite (SiO_2). Upon firing at 1100 °C, diffraction peaks corresponding to mullite ($3Al_2O_3{\cdot}2SiO_2$) become clearly evident (Fig. 11g). The development of mullite, a mechanically stable aluminosilicate phase, is consistent with the highest compressive strength recorded for the control specimens.

Introducing CBA leads to distinct mineralogical changes. In the modified bricks (10 and 40 wt.% CBA), additional peaks associated with albite ($NaAlSi_3O_8$) are detected alongside quartz, hematite, and cristobalite. As the CBA content increases to 40 wt.%, the overall peak intensity decreases. This behavior is plausibly related to the high alkali and alkaline-earth oxide contents in CBA (notably Na_2O and CaO), which favor albite formation and enhance fluxing. Albite acts as a potent fluxing phase that promotes early liquid-phase (glassy) formation at elevated temperatures; the resulting melt tends to partially dissolve other crystalline phases, thereby reducing the relative intensities of other diffraction peaks compared with those of the control bricks.

Mullite peaks are also detected in CBA-containing specimens even at 900 °C, suggesting that part of the mullite is inherited directly from the original bottom ash (formed during high-temperature coal combustion) rather than being entirely neo-formed during brick firing [27]. This inherited mullite framework, together with the albite-assisted liquid phase, governs the sintering behavior and contributes to the composite bricks observed physical and mechanical properties [28-29].

SEM observations were performed on the fractured surfaces of representative specimens to clarify the relationship between physical–mechanical behavior and internal structure (Fig. 12). The control bricks (0 wt.% CBA) exhibit a relatively dense, compact microstructure, particularly at 1100 °C, indicating advanced vitrification and adequate particle bonding. With the addition of the CBA, the morphology shifts markedly toward a more porous texture. Bricks with high CBA content (40 wt.% CBA) exhibit a sponge-like structure with large, interconnected voids (Fig. 12c, f, and i).

This extensive porosity arises from two gas-forming mechanisms during firing: combustion of residual carbon in the ash (LOI 5.56%) and thermal decomposition of sulfate-bearing compounds (SO_3 3.32%). The evolution of CO_2 and SO_x generates internal pressure that forms vesicles and promotes bloating within the ceramic matrix, while limited viscous flow at lower firing temperatures restricts gas escape and results in large, interconnected pores [30].

5. CONCLUSION

This study systematically assessed the feasibility of recycling coal bottom ash (CBA) as a supplementary raw material for fired clay bricks. From the physical, mechanical, and microstructural investigations, the following conclusions can be drawn.

1. Incorporating CBA reduced bulk density steadily, indicating potential for lightweight masonry units. However, higher CBA contents increased water absorption and apparent porosity. SEM observations confirmed a porous, sponge-like structure at high CBA loadings, primarily due to gas release from residual carbon combustion and sulfate decomposition during firing.

2. XRD analyses showed that sintering of CBA–clay bricks is controlled by flux-assisted liquid-phase formation. Albite, promoted by the alkali-rich CBA, contributed to partial vitrification at elevated temperatures. Mullite peaks detected even at lower firing temperatures indicate a partly inherited mullite framework from the original ash, which acts as a refractory skeleton during firing.

3. Compressive strength decreased with increasing CBA due to the pore-forming effect, but raising the firing temperature to 1000–1100 °C significantly improved densification and compensated for strength loss. The optimal range was 10–30 wt.% CBA fired at ≥1000 °C, which achieved compressive strengths above the 17.2 MPa ASTM C62 requirement for moderate weathering (MW) grade bricks.

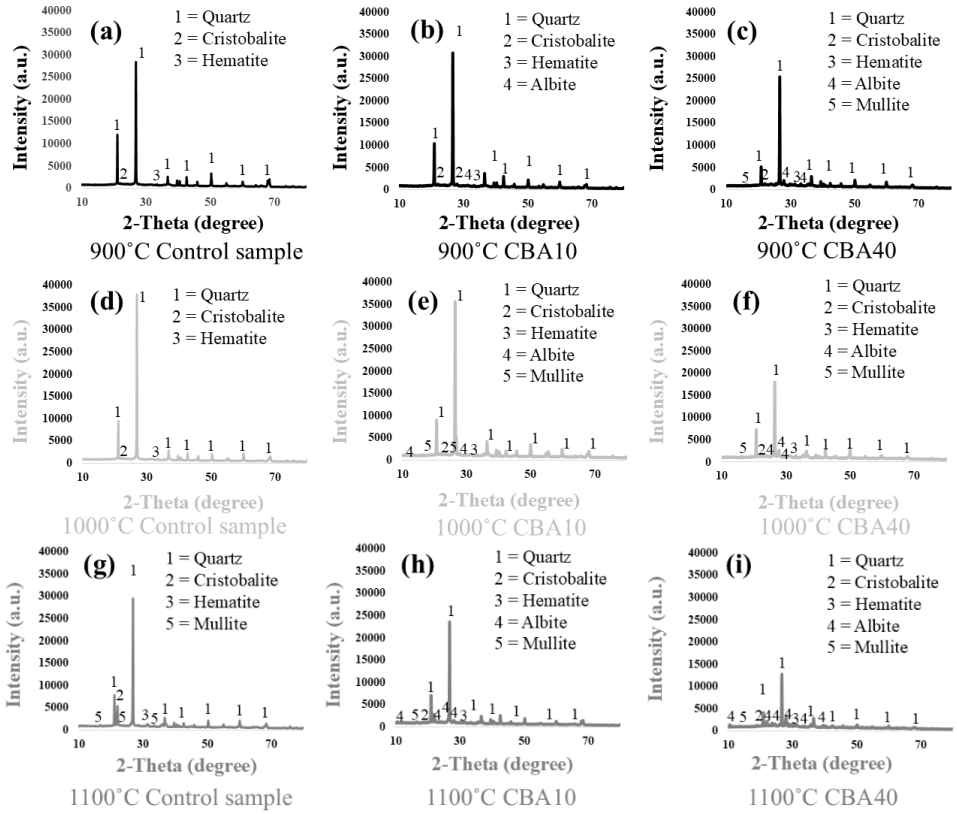

Fig. 11 XRD patterns of clay bricks incorporating 10–40 wt.% CBA fired at 900, 1000, and 1100 °C.

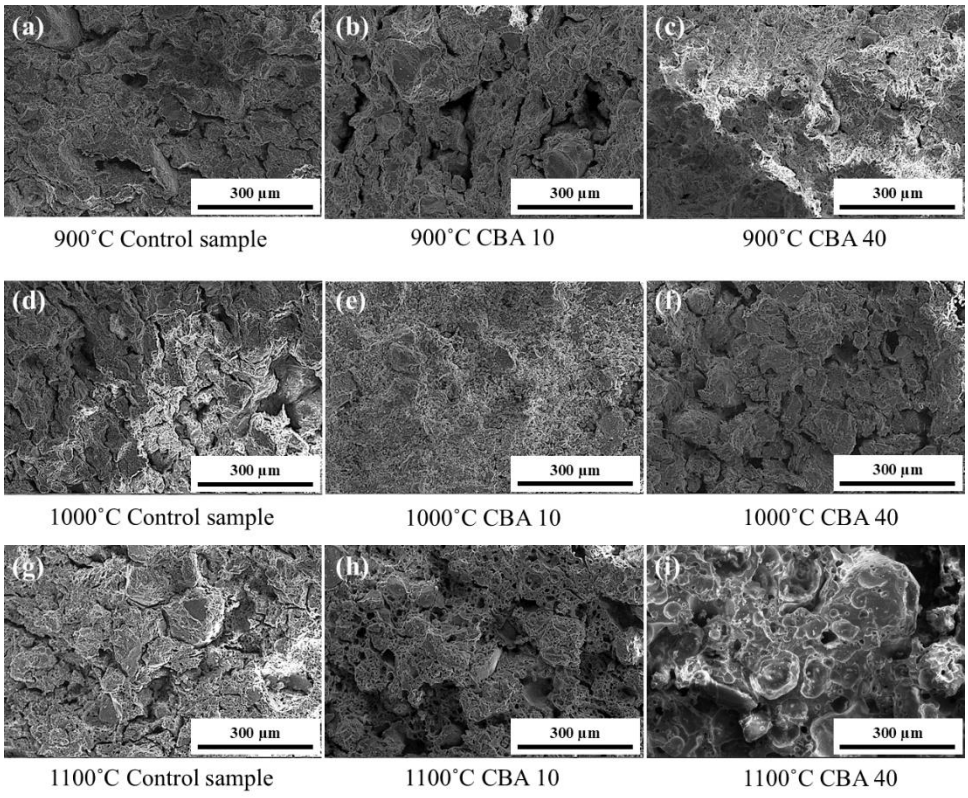

Fig. 12 SEM micrographs illustrating pore evolution and glassy-phase development in CBA-modified clay bricks with 10 wt.% and 40 wt.% substitutions, fired at 900, 1000, and 1100 °C.

4. Overall, the results demonstrate that CBA can be effectively valorized to produce durable fired bricks, reducing natural clay consumption and providing a practical route for coal-waste management in line with circular economy principles, without compromising compliance with technical standards.

6. ACKNOWLEDGMENTS

This project is supported by Thailand Science Research and Innovation (TSRI), which allocated a budget through the National Science, Research, and Innovation Fund (NSRF), Rajabhat Maha Sarakham University, FRB690009/0208/11.

7. REFERENCES

1. Muñoz P., Letelier V., Muñoz L., Bustamant M. A., Gencel O., and Sutcu M., The combined effect of bottom ashes and cellulose fibers on fired clay bricks. Construction and Building Materials, Vol. 301, 2021, pp.124307.
2. Sameer H., and Bringezu S., Life cycle input indicators of material resource use for enhancing sustainability assessment schemes of building. Journal of Building Engineering, Vol. 21, 2019, pp.230-242.
3. Pitak I., Baltušnilas A., Kalpokaitė-Dičkuvienė R., Kriukiene R., and Denafas G., Experimental study effect of bottom ash and temperature of firing on the properties, microstructure and pore size distribution of clay bricks: A Lithuania point of view. Case Studies in Construction Materials, Vol. 17, 2022, pp. e01230.
4. Taurino R., Karamanova E., Barbieri L., Atanasova-Vladimirova F., and Karamanov A., New fired bricks based on municipal solid waste incinerator bottom ash. Waste Management & Research, Vol. 35 (10), 2017, pp. 1-9.
5. Dhanapandian S., and Gnanavel B., Using granite and marble sawing power waste in the production of bricks: Spectroscopic and mechanical analysis. Research Journal of Applied Sciences, Engineering and Technology, Vol. 2 (1), 2010, pp. 73-86.
6. Aeslina A. K., Abbas M., Felicity R., and John B., Density, strength, thermal conductivity and leachate characteristics of light weight fired clay bricks incorporating cigarette butts. International Journal of Civil and Environmental Engineering, Vol. 2, 2010, pp. 179-184.
7. Sahu M. K., and Singh L., Critical review on types of bricks type 5: Common burnt clay bricks. International Journal of Mechanical and Production Engineering, Vol. 5 (11), 2017, pp. 120-123.
8. Ghisellini P., Ripa M., and Ulgiati S., Exploring environmental and economic costs and benefits of a circular economy approach to the construction and demolition sector A literature review. Journal of Cleaner Production, Vol. 178, 2018, pp. 618-643.
9. Kaushik H. B., Rai D. C., and Jain S. K., Stress-strain characteristics of clay brick masonry under uniaxial compression. Journal of Materials in Civil Engineering, Vol 19 (9), 2007, pp. 728-739.
10. Ramakrishnan K., Chellappa and V., Chandrasekarabarathi S., Manufacturing of low-cost bricks using waste materials. Materials Proceedings, Vol. 13 (25), 2023, pp. 1-8.
11. Brown A., Bricks: a review of sustainability and toxicity issues. Sustainability and Toxicity of Building Materials, 2024, pp. 179-194.
12. Mohammed B. S., and Al-Ebrahimy S. N., Production of lightweight clay bricks using polymer waste. Engineering and Technology Journal, Vol. 38, 2018, pp. 823-831.
13. Adediran A., Kikky S. M., Adhikary S. K, Ducman V., and Perumal P., Upcycling municipal solid waste incineration bottom ash in clay-bonded bricks. 2024, Article in Press.
14. Kizinievič O., Voišnienė V., Kizinievič V., and Pundienė I., Impact of municipal solid waste incineration bottom ash on the properties and frost resistance of clay bricks. Journal of Material Cycles and Waste Management. Vol. 24, 2022, pp. 237-249.
15. Sutcu M., Erdogmus E., Gencel O., Gholampour A., Atan E., and Ozbakkaloglu T., Recycling of bottom ash and fly ash wastes in eco-friendly clay brick production. Journal of Cleaner Production. Vol. 233, 2019, pp. 753-764.
16. ASTM C326-09., Standard Test Method for Drying and Firing Shrinkages of Ceramic Whiteware Clays. West Conshohocken, Pennsylvania. ASTM Book of Standards 15.02, 2018.
17. ASTM C373-18., Standard Test Method for Water Absorption, Bulk Density, Apparent Porosity, and Apparent Specific Gravity of Fired Whiteware Products, Ceramic Tiles, and Glass Tiles. West Conshohocken, Pennsylvania. ASTM Book of Standards 15.02, 2018.
18. ASTM C773-88., Standard Test Method for Compressive (Crushing) Strength of Fired Whiteware Materials, West Conshohocken, Pennsylvania. ASTM Book of Standards. 15.02, 2020.
19. ASTM D422-63., Standard test method for Particle-Size Analysis of Soils. West Conshohocken, Pennsylvania. ASTM Book of standards. 2007.

20. Chindaprasirt P., Srisuwan A., Saengthong C., Lawanwadeekul S., and Phonphuak N., Synergistic effect of fly ash and glass cullet additive on properties of fire clay bricks. Journal of Building Engineering. Vol. 44, 2022, pp. 128327.
21. Ozturk S., Sutcu M., Erdogmus E., and Gencel O., Influence of tea waste concentration in the physical, mechanical and thermal properties of brick clay mixtures. Construction and Building Materials. Vol. 217, 2019, pp. 592-599.
22. Saraphirom P., Namsena P., Teerakun M., Phonphuak S., Chanprathak A., Dakaew S., and Phonphuak P., Development of fired clay granules as eco-friendly substances for nitrogen-fixing bacterial cells. International Journal of GEOMATE, vol. 27, No. 120, 2024, pp.110-121.
23. Lawanwadeekul S., Otsuru T., Tomiku R., and Nishiguchi H., Thermal-acoustic clay brick production with added charcoal for use in Thailand. Construction and Building Materials, Vol. 255, 2020, pp. 119376.
24. Phonphuak, N., Application of Dry Grass for Clay Brick Manufacturing. Key Engineering Materials, Vol. 757, 2017, pp. 35-39.
25. Phonphuak, N., Teerakun, M., Srisuwan, A., Ruenruangrit, P., and Saraphirom, P., The use of sawdust waste on physical properties and thermal conductivity of fired clay brick. International Journal of GEOMATE, Vol. 18, No. 69, 2020, pp. 24- 29.
26. ASTM C62-23., Standard specification for building brick (solid masonry units made from clay or shale). ASTM International. https://www.astm.org/c0062-23.html
27. Lawanwadeekul, S., Chindaprasirt, P., Phumiphan, A., Srisuwan, A. and Phonphuak, N. (2025). Transforming industrial waste by utilizing fly ash and bottom ash for sustainable clay bricks. Journal of Material Cycles and Waste Management, 27(5), 3480-3494.
28. Srisuwan, A., Lawanwadeekul, S., Saengthong, C., Artbumrung, S., and Phonphuak, N., Effects of fly ash addition on the durability and mechanical performance of fired clay bricks. Suranaree Journal of Science and Technology, 29(1), 2022, 010095(1–6).
29. Lawanwadeekul, S., Chindaprasirt, P., Ariyajinno, N., Srisuwan, A., and Phonphuak, N., Acid-resistant clay bricks incorporating bottom ash and waste glass strengthened by mullite suppression and albite formation, Next Materials, Vol. 11, 2026, Article 101610.
30. Sokolař, R., & Nguyen, M. (2019). Sulphur dioxide emissions during the firing of ceramic bodies based on class C fly ash. Solid State Phenomena, 296, 149-154. https://doi.org/10.4028/www.scientific.net/SSP.296.149